 doi:10.20944/preprints202110.0117.v1

Article

HIF-α activation impacts macrophage function during murine *Leishmania major* infection.

Manjunath Bettadapura[1], Hayden Roys[1], Anne Bowlin[1], Gopinath Venugopal[1], Charity L. Washam[2,3], Lucy Fry[1], Steven Murdock[1], Humphrey Wanjala[1], Stephanie D. Byrum[2,3], and Tiffany Weinkopff[1,*]

[1] Department of Microbiology and Immunology, College of Medicine, University of Arkansas for Medical Sciences, Little Rock, AR, USA 72205; mnbettadapur@ualr.edu (M.B), hroys@uams.edu (H.R.), abowlin@uams.edu (A.B.), gvenugopal@uams.edu (G.V.), lfry@uams.edu (L.F.), sjmurdock@uams.edu (S.M.), hmwanjala@ular.edu (H.W.), and tweinkopff@uams.edu (T.W.)

[2] Department of Biochemistry and Molecular Biology, College of Medicine, University of Arkansas for Medical Sciences, Little Rock, AR, USA 72205; cwasham@uams.edu (C.L.W.), and sbyrum@uams.edu (S.D.B.),

[3] Arkansas Children's Research Institute, Little Rock, AR, USA 72202

***** Correspondence: tweinkopff@uams.edu; 501-686-5518

Abstract: Leishmanial skin lesions are characterized by inflammatory hypoxia alongside the activation of hypoxia inducible factors, HIF-1α and HIF-2α, and subsequent expression of the HIF-α target VEGF-A during *Leishmania major* infection. However, the factors responsible for HIF-α activation are not known. We hypothesize hypoxia and pro-inflammatory stimuli contribute to HIF-α activation during infection. RNASeq on leishmanial lesions found transcripts associated with HIF-1α signaling are induced. To determine whether hypoxia contributes to HIF-α activation, we followed the fate of myeloid cells infiltrating from the blood and into hypoxic lesions. Recruited myeloid cells experience hypoxia when they enter inflamed lesions, and the length of time in lesions increases their hypoxic signature. To determine whether pro-inflammatory stimuli in the inflamed tissue can also influence HIF-α activation, we subjected macrophages to various pro-inflammatory stimuli and measured VEGF-A. While parasites alone did not induce VEGF-A, and pro-inflammatory stimuli only modestly induce VEGF-A, HIF-α stabilization increases VEGF-A during infection. HIF-α stabilization does not impact parasite entry, growth or killing. Alternatively, the absence of ARNT/HIF-α signaling enhances parasite internalization. Altogether, these findings suggest HIF-α is active during infection, and while macrophage HIF-α activation promotes lymphatic remodeling through VEGF-A production, HIF-α activation does not impact parasite internalization or control.

Keywords: Leishmania; leishmaniasis; macrophages; HIF-α

1. Introduction

Leishmaniasis is an inflammatory disease caused by the vector-borne, obligate intracellular protozoan parasites of the genus *Leishmania*. Leishmaniasis is endemic in many developing countries in the tropical and subtropical regions of the globe, where up to 1.7 million new cases in 98 countries occur annually [1, 2]. *Leishmania* manifests in three forms: 1) visceral leishmaniasis (VL), which is systemic and fatal if untreated, 2) cutaneous leishmaniasis (CL), which causes nodules, papules and lesions on the surface of the skin, and 3) mucocutaneous leishmaniasis (MCL), wherein parasites from a primary cutaneous lesions spread to other parts of the body [3]. Infections by different species of *Leishmania* manifest in different clinical forms. In particular, *Leishmania major* is responsible for CL in the Eastern Mediterranean and North Africa where the disease is considered a major public health problem and accounts for 70% of the CL cases worldwide [4]. The burden on these countries, already high due to current socio-economic conditions, limited resources and medical infrastructure, and civil strife, is further exacerbated by the lack of a vaccine and ineffective chemotherapeutic treatment for the disease [3, 4].

The transcription factor hypoxia inducible factor-1α (HIF-1α), which is involved in cellular stress and the response to decreased oxygen availability, is present in lesions from humans and mice infected with *Leishmania* parasites [5-8]. The disease severity is also associated with enhanced levels of HIF-1α in human and murine CL [6, 8]. We previously reported target genes of HIF-1α as well as HIF-2α are elevated following *L. major* infection in vivo [6, 8, 9]. These data suggest both HIF-1α and HIF-2α are active in

Preprints (www.preprints.org) | NOT PEER-REVIEWED | Posted: 7 October 2021 doi:10.20944/preprints202110.0117.v1

the skin during CL. Moreover, HIF-1α and the downstream target gene, VEGF-A, are elevated in infected and uninfected macrophages in the lesions [8]. Even though other species of *Leishmania* parasites activate HIF-1α [10, 11], *L. major* parasites alone do not induce HIF-1α accumulation or target gene expression in macrophages [6]. In contrast, infected macrophages cultured under hypoxic conditions or stimulated with pro-inflammatory signals like IFNγ and LPS enhanced HIF-1α activation [6]. HIF-1α activated by these inflammatory signals promoted leishmanicidal macrophage activity, but HIF-1α stabilization alone in the absence of inflammatory signals did not promote parasite killing [6]. Altogether, these data suggest the tissue microenvironment, rather than the parasites, drive pan-HIF-α activation during *L. major* infection.

Macrophages perform multiple functions in the skin following *L. major* infection. Macrophages play an essential role in antileishmanial immunity by recognizing, phagocytosing and killing parasites [3]. In addition to phagocytosing parasites, dermal macrophages also phagocytose apoptotic cells and debris as part of the wound healing response [12, 13]. Even though macrophages present antigen in other infections, *Leishmania* infection in macrophages impairs antigen presentation and IL-12 release thereby dampening $CD4^+$ Th1 immune responses [14-17]. During an efficient antileishmanial immune response, $CD4^+$ Th1 cells produce IFNγ that signals to macrophages to kill parasites in an NO- and ROS-dependent manner which ultimately lead to parasite control and lesion resolution [3]. While the importance of macrophages in the immune response has been well-characterized, recent evidence has shown macrophages also play a role in vascular remodeling at the site of infection [8]. Macrophages produce VEGF-A which binds to VEGFR-2 on lymphatic endothelial cells to induce lymphangiogenesis [7, 8]. Macrophage VEGF-A is dependent on HIF-α signaling and mice deficient in myeloid pan-HIF-α signaling exhibit increased pathology [8]. Therefore, in addition to their well-characterized role in immune responses and parasite killing, macrophages also orchestrate the expansion of the lymphatics which leads to lesion resolution during *L. major* infection.

Given HIF-1α and HIF-2α are activated in leishmanial lesions [6-8, 18], and macrophage HIF-α activation contributes to lesion resolution [8], we investigated factors contributing to HIF-α activation as well as other downstream consequences of HIF-α activation during *L. major* infection. We developed an in vitro system where HIF-α is constitutively active by exposing macrophages to dimethyloxalylglycine (DMOG), a chemical agent that inhibits the prolyl-4-hydroxylase domain (PHD) enzymes that degrade HIF-α isoforms, thereby stabilizing HIF-α over the course of infection [19]. Therefore, macrophage DMOG treatment mimics HIF-1α and HIF-2α activation detected in leishmanial lesions. Using this system, we found HIF-α activation does not impact parasite entry or control, but rather that basal HIF-α signaling restricts parasite internalization by macrophages.

2. Results

2.1 The HIF-1α signaling pathway is increased during L. major infection in vivo

Leishmanial lesions in the skin are characterized by inflammatory hypoxia. To determine if hypoxia at the site of infection is associated with increased HIF-α signaling during *L. major* infection in the murine model, we infected C57BL/6 mice with *L. major* parasites. At 4 weeks p.i. when mice presented with lesions, we performed RNASeq on infected and control uninfected ears from naïve mice. Differentially expressed genes (DEGs) between infected and naïve ears were identified by Limma voomWithQualityWeights in R, and pathway enrichment analysis of DEGs was performed using EGSEA against the KEGG database. The gene expression profiles derived from the RNASeq data were considered statistically significant with a fold change >2 and $p<0.05$. Hierarchical clustering analysis reveals many transcripts that were significantly induced following *L. major* infection are associated with the HIF-1α signaling pathway including *Egln1 (Phd2), Egln3, (Phd3), Eno2, Hif1a, Hk2, Hk3, Ldha, Nos2, Vegfa*, and *Vhl* (Figure 1). Altogether, our global transcriptomic analysis suggests HIF-1α signaling is increased during *L. major* infection in vivo, consistent with findings that leishmanial lesions are hypoxic.

Preprints (www.preprints.org) | NOT PEER-REVIEWED | Posted: 7 October 2021 doi:10.20944/preprints202110.0117.v1

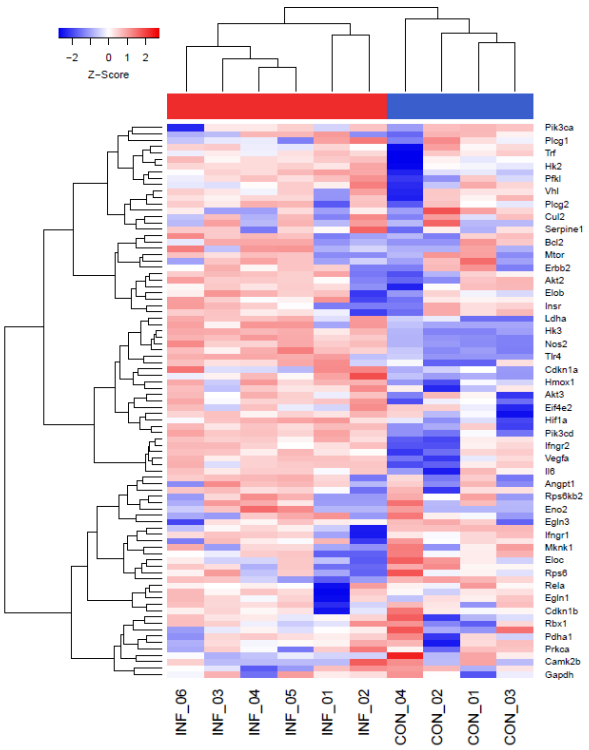

Figure 1: The HIF-1α signaling pathway is elevated following with infection with L. major parasites in vivo. C57BL/6 mice were infected with 2x10^6 *L. major* metacyclic promastigote parasites intradermally in the ear. At 4 weeks p.i., naïve control (N=4) and infected (N=6) ears were subjected to RNASeq analysis. Hierarchical clustering of the expression profile was performed. Heat maps indicate the fold change of gene expression in *L. major*-infected ears >2-fold (red) or <2-fold (blue) compared to naïve controls. The HIF-1α signaling pathway was obtained using the KEGG pathway analysis database. Relative expression was normalized with a Z score.

2.2 Myeloid cells experience inflammatory hypoxia in leishmanial lesions

We hypothesize inflammatory hypoxia further potentiates chronic inflammation in leishmanial lesions. We previously reported inflammatory monocytes, which are massively recruited to the site of infection following *L. major* inoculation, are less hypoxic at the cellular level compared to macrophages in the skin during infection [9]. However, it was not clear whether this was a cell intrinsic feature that distinguishes monocytes from macrophages, or if the tissue microenvironment imprints a hypoxic signature upon these cells. Therefore, we utilized an adoptive transfer system where CD11b$^+$ cells isolated from the bone marrow of CD45.1 donor mice were injected into CD45.2 recipient mice that were infected 4 weeks prior to the cell transfer with *L. major* parasites. Infected mice were then treated with pimonidazole to determine which cells are experiencing hypoxic conditions at the cellular level (Figure 2A). For most studies, hypoxia is detected at the tissue level; however, this adoptive transfer model examines hypoxia at a higher resolution and determines if monocytes can become hypoxic as they enter inflamed tissues at the cellular level. Using this system coupled with flow cytometry, we found CD45.1$^+$CD11b$^+$ cells are detectable in the lesions of infected CD45.2$^+$ mice suggesting myeloid cells are actively recruited to the site of infection (Figure 2B). Further analysis of the transferred myeloid cells from the donor mouse present at the site of infection showed the CD45.1$^+$ cells displayed a CD11b$^+$Ly6G$^+$ neutrophil or CD11b$^+$Ly6G$^-$CD64$^+$ macrophage phenotype. Confirming previous results, these data suggest monocytes differentiate into macrophages following *Leishmania* infection [20-22]. The amount of hypoxia staining based on the pimonidazole median fluorescence intensity (MFI) for each myeloid cell type from the donor CD45.1$^+$ cells as well as the endogenous host CD45.2$^+$ cells was investigated (Figure 2C). These studies revealed CD11b$^+$Ly6G$^+$ neutrophils exhibited lower levels of pimonidazole staining compared to macrophages in both the CD45.2$^+$ host and CD45.1$^+$ transferred cells. Importantly, macrophages derived from CD45.1$^+$ donor mice possessed similar pimonidazole MFIs compared the CD45.2$^+$ endogenous macrophages (Figure 2D). These data suggest monocyte-derived macrophages recruited

Preprints (www.preprints.org) | NOT PEER-REVIEWED | Posted: 7 October 2021 doi:10.20944/preprints202110.0117.v1

from the circulation experience hypoxic conditions in the inflamed lesions which may impact their metabolic reprogramming, and thus the differentiation or function of that cell.

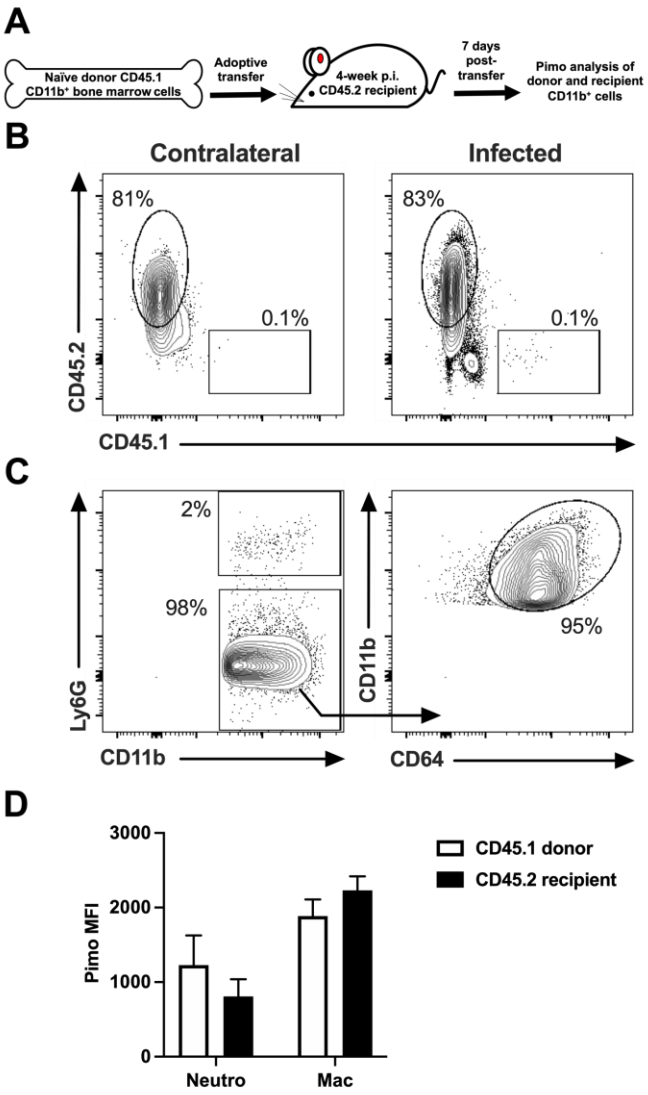

Figure 2. Myeloid cells experience inflammatory hypoxia as they enter the dermal tissue during L. major infection. C57BL/6 mice were infected with *L. major* parasites intradermally in the ear. At 4 weeks post-infection, CD45.1$^+$CD11b$^+$ cells isolated from the bone marrow of naïve mice were adoptively transferred retroorbitally into CD45.2$^+$ infected mice. At 7 days post-transfer, infected mice were given pimonidazole i.p. 90 min before euthanizing, and cells from infected ears were stained for pimonidazole and analyzed by flow cytometry. **(A)** Cartoon model of CD11b$^+$ adoptive transfer experiment. **(B)** Representative dot plots showing CD45.1$^+$ transferred cells are present in infected ears of CD45.2$^+$ recipient mice. Cells were previously gated on total, live singlet events. **(C)** Representative dot plots showing flow cytometry gating strategy for CD11b$^+$Ly6G$^+$ neutrophils and CD11b$^+$Ly6G$^-$ CD64$^+$ macrophages. **(D)** Quantification of Pimonidazole (pimo) median fluorescence intensity (MFI) after gating on the myeloid cells: CD11b$^+$Ly6G$^+$ neutrophils and CD11b$^+$Ly6G$^-$CD64$^+$ macrophages. Data shown here from one experiment and representative of two independent experiments with 5 mice per group. Data are presented as the mean +SEM with no significant differences in pimonidazole MFIs between donor cells and endogenous host cells of the same cell type as analyzed by a paired *t-test*.

2.3 The length of time a myeloid cell spends in leishmanial lesions dictates the hypoxic signature of that cell

Following *L. major* infection, monocytes migrate into lesions and exhibit a hypoxic signature, but the length of time in the inflamed tissue may influence the hypoxic signature of the cell furthering impacting myeloid cell differentiation and function. To determine if increased time in the lesion enhances hypoxia at the cellular level, we investigated myeloid

Preprints (www.preprints.org) | NOT PEER-REVIEWED | Posted: 7 October 2021 doi:10.20944/preprints202110.0117.v1

cells at different stages of their transition from monocytes to macrophages based on the downregulation of Ly6C (an inflammatory monocyte marker) and upregulation of CD64 (a macrophage marker) (Figure 3A). This strategy examining myeloid cells that are actively differentiating from Ly6C^{hi}CD64^{-} inflammatory monocytes to Ly6C^{-}CD64^{+} macrophages coupled with pimonidazole staining determined hypoxia at the cellular level across the stages of transition. Confirming previous work [9], we found Ly6C^{hi}CD64^{-} inflammatory monocytes exhibited less pimonidazole staining than Ly6C^{-}CD64^{+} fully differentiated macrophages (Figure 3B-C). Moreover, Ly6C^{hi}CD64^{-} inflammatory monocytes have decreased pimonidazole stain, and as monocytes transition to Ly6C^{hi}CD64^{+} cells, their pimonidazole stain positivity also increases. The trend continues where Ly6C^{lo}CD64^{+} cells have higher levels of pimonidazole compared to Ly6C^{hi}CD64^{+} cells, that eventually peaks in the Ly6C^{-}CD64^{+} macrophages which have the greatest pimonidazole MFI (Figure 3B-C). These data suggest inflammatory monocytes that enter the inflamed tissue experience hypoxic conditions, and the length of time in the lesion imprints a hypoxic signature upon these cells as they differentiate into macrophages.

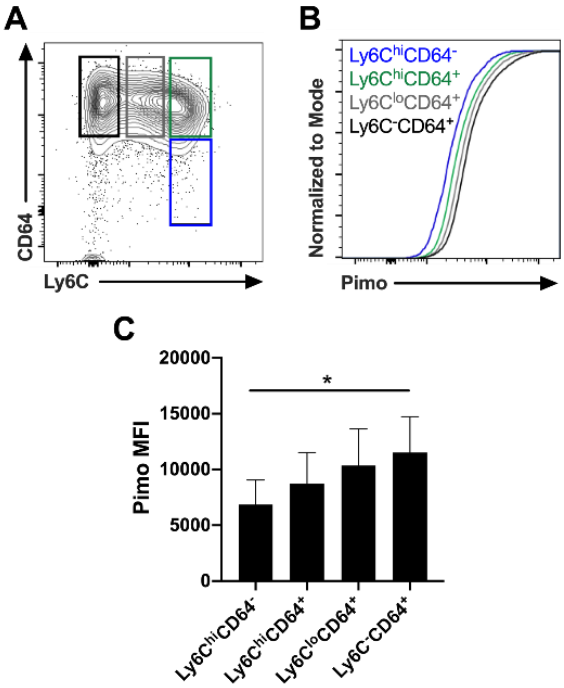

Figure 3. Myeloid cell longevity in the dermal tissue is associated with inflammatory hypoxia during L. major infection. C57BL/6 mice were infected with *L. major* parasites intradermally in the ear. At 5 weeks post-infection, mice were given pimonidazole i.p. 90 min before euthanizing, and infected ears were stained for pimonidazole and analyzed by flow cytometry. **(A)** Representative flow cytometry contour plot showing subpopulations in the monocyte to macrophage transition from Ly6C^{hi}CD64^{-} inflammatory monocytes to Ly6C^{-}CD64^{+} macrophages after gating on total, live, singlet, and CD45^{+}CD11b^{+}Ly6G^{-} cells. **(B)** Representative flow cytometry cumulative distribution function (CDF) plot showing pimonidazole MFI after gating on the myeloid Ly6C^{hi}CD64^{-}, Ly6C^{hi}CD64^{+} cells, Ly6C^{lo}CD64^{+} cells, and Ly6C^{-}CD64^{+} subpopulations in figure A. **(C)** Quantification of pimonidazole MFI in myeloid subpopulations from infected skin from figure B. Data shown here from one experiment and representative of two independent experiments with 5 mice per group. Data are presented as the mean +SEM. *$p < 0.05$, one-way ANOVA followed by the post hoc Tukey's test comparing pimonidazole MFI between all subpopulations.

2.4 Proinflammatory stimuli and HIF-α stabilization induce macrophage VEGF-A production in an ARNT/HIF-dependent manner during L. major infection

To determine whether additional pro-inflammatory stimuli present at the site of infection could also activate HIF-α in addition to hypoxia during infection, we established an in vitro culture system using BMDMs. Macrophages were cultured alone or with a panel of pro-inflammatory stimuli including LPS and IFNγ in the presence or absence of DMOG to stabilize HIF-1α and HIF-2α. These conditions in conjunction with *L. major* infection in macrophages mimic the hypoxic environment and elevated HIF-1α and HIF-2α expression present at the site of infection in leishmanial lesions [9]. Specifically, macrophages were

Preprints (www.preprints.org) | NOT PEER-REVIEWED | Posted: 7 October 2021 doi:10.20944/preprints202110.0117.v1

cultured with LPS alone, IFNγ alone, or in combination, in macrophages that were infected or not with *L. major* parasites (5:1 MOI). Compared to uninfected control macrophages, infection with *L. major* parasites alone did not induce VEGF-A production after 24 hours (Figure 4A). Amongst uninfected macrophages, only the combination of LPS/IFNγ resulted in significant VEGF-A production (Figure 4A). In infected macrophages, the addition of LPS or LPS/IFNγ led to significant VEGF-A production (Figure 4A). Importantly, VEGF-A production was significantly elevated in all conditions with the addition of DMOG, when comparing the same condition with and without DMOG (Figure 4A).

To confirm that DMOG stabilizes HIF-α leading to HIF-α activation during infection, VEGF-A production was measured from BMDMs generated from LysM^{Cre}ARNT$^{f/f}$ which are deficient in myeloid ARNT/HIF-α signaling and LysM^{Cre}ARNT$^{f/+}$ control mice which exhibit intact ARNT/HIF-α signaling. Using these genetic mouse models demonstrates DMOG treatment is directly affecting ARNT/HIF-α signaling, and not acting as an off target effect. Compared to macrophages from LysM^{Cre}ARNT$^{f/+}$ mice, LysM^{Cre}ARNT$^{f/f}$ macrophages produced significantly less basal VEGF-A (Figure 4A-B). In LysM^{Cre}ARNT$^{f/f}$ macrophages only LPS plus parasites led to significant VEGF-A production that did not increase with DMOG suggesting some VEGF-A production during infection can be independent of ARNT/HIF-α signaling (Figure 4B). Importantly, LysM^{Cre}ARNT$^{f/f}$ macrophages produced significantly less VEGF-A compared to LysM^{Cre}ARNT$^{f/+}$ macrophages in the presence of DMOG for all conditions (Figure 4A-B). Altogether these results suggest that some pro-inflammatory stimuli present in leishmanial lesions could activate HIF-α, but the overall effects of the pro-inflammatory stimuli tested are modest compared to chemical stabilization of HIF-1α and HIF-2α.

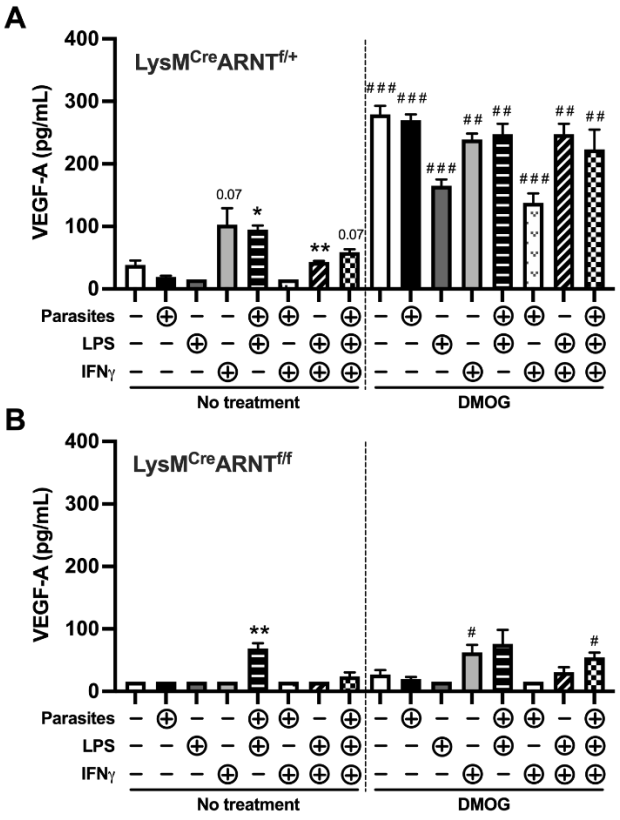

Figure 4. Macrophages produce VEGF-A in response to proinflammatory stimuli and HIF-α stabilization during L. major infection in an ARNT/HIF-dependent manner. BMDMs were cultured with LPS (100 ng/mL) alone, IFNγ (10 ng/mL) alone, or in combination, in macrophages that were infected or not with *L. major* parasites (5:1 MOI). BMDMs were also cultured under these conditions with and without 0.2 mM DMOG which stabilizes HIF-α. BMDMs were generated from **(A)** LysM^{Cre}ARNT$^{f/+}$ or **(B)** LysM^{Cre}ARNT$^{f/f}$ to determine to contribution of ARNT/HIF signaling for VEGF-A production. Supernatants were collected after 24 hours. VEGF-A production was quantified by ELISA. Data are presented as mean +SEM. $^{**}p < 0.01$, $^{*}p < 0.05$, *t-test* comparing proinflammatory stimuli to media alone; # # # $p < 0.005$, # # $p < 0.01$, *t-test* comparing the same treatment condition with and without DMOG. Even though not depicted in the figure, it should be noted all

Preprints (www.preprints.org) | NOT PEER-REVIEWED | Posted: 7 October 2021 doi:10.20944/preprints202110.0117.v1

LysM^{Cre}ARNT$^{f/+}$ BMDMs treated with DMOG produced significantly more VEGF-A than LysM^{Cre}ARNT$^{f/f}$ BMDMs treated with DMOG ($p < 0.01$ by *t-test* comparing different mouse strains exposed to the same condition).

2.5 DMOG induces HIF-1α and HIF-2α activation during L. major infection

During *L. major* infection in vivo, HIF-1α and HIF-2α as well as multiple HIF-1α and HIF-2α targets including *Vegfa*, *Nos2*, and *Arg1* and are elevated at the site of infection [7, 8, 18]. To determine the effects of pan-HIF-α stabilization during *L. major* infection, we stimulated BMDMs in the presence of DMOG to mimic HIF-1α and HIF-2α stabilization in vitro. Macrophages were generated from LysM^{Cre}ARNT$^{f/f}$ and LysM^{Cre}ARNT$^{f/+}$ mice to determine the requirement for myeloid HIF-α signaling in response to DMOG administration. Macrophages were exposed to 0.1 or 0.2 mM DMOG prior to infection and the expression of VEGF-A which can result from HIF-1α or HIF-2α activation was examined by real-time PCR. Our results show *L. major* parasites alone do not induce VEGF-A expression in LysM^{Cre}ARNT$^{f/+}$ macrophages (Figure 5A), confirming previous findings [9]. However, DMOG exposure in infected and uninfected macrophages upregulated *Vegfa*, confirming results in Figure 4. Importantly, VEGF-A expression was lower in LysM^{Cre}ARNT$^{f/f}$ macrophages compared to LysM^{Cre}ARNT$^{f/+}$ control BMDMs during *L. major* infection in response to DMOG, suggesting HIF-α mediates *Vegfa* expression during infection. In addition, HIF-1α-specific and HIF-2α-specific target genes were examined during infection in BMDMs treated or not with DMOG. As with *Vegfa,* the expression of HIF-1α-specific targets *Nos2* and *Pgk1* was significantly higher in uninfected DMOG-treated LysM^{Cre}ARNT$^{f/+}$ macrophages compared to untreated LysM^{Cre}ARNT$^{f/+}$ controls, but the same trend was not seen in LysM^{Cre}ARNT$^{f/f}$ macrophages (Figure 5B-C). While DMOG increased both HIF-1α-specific targets *Nos2* and *Pgk1* in LysM^{Cre}ARNT$^{f/+}$ macrophages compared to untreated cells during infection, this effect was only significant for *Nos2* expression (Figure 5B-C). Importantly, there was no significant difference detected in HIF-1α targets *Nos2* and *Pgk1* in LysM^{Cre}ARNT$^{f/f}$ macrophages with DMOG treatment compared to untreated cells (Figure 5B-C). The expression of HIF-2α-specific target *Arg1* was significantly higher in both uninfected and infected LysM^{Cre}ARNT$^{f/+}$ macrophages with DMOG treatment compared to untreated LysM^{Cre}ARNT$^{f/+}$ macrophages (Figure 5D). While Arg1 was not significantly elevated in LysM^{Cre}ARNT$^{f/f}$ macrophages with DMOG treatment, some increased Arg1 was detected in uninfected LysM^{Cre}ARNT$^{f/f}$ macrophages suggesting some DMOG-induced *Arg1* is independent of ARNT/HIF-α signaling (Figure 5D). The expression of HIF-2α-specific target *Epo* was higher in both uninfected and infected LysM^{Cre}ARNT$^{f/+}$ macrophages with DMOG treatment compared to untreated LysM^{Cre}ARNT$^{f/+}$ macrophages, but this result was not significant (Figure 5E). Altogether, these data indicate that DMOG is an effective tool to simulate *Vegfa* and other HIF-α targets during *L. major* infection.

Preprints (www.preprints.org) | NOT PEER-REVIEWED | Posted: 7 October 2021 doi:10.20944/preprints202110.0117.v1

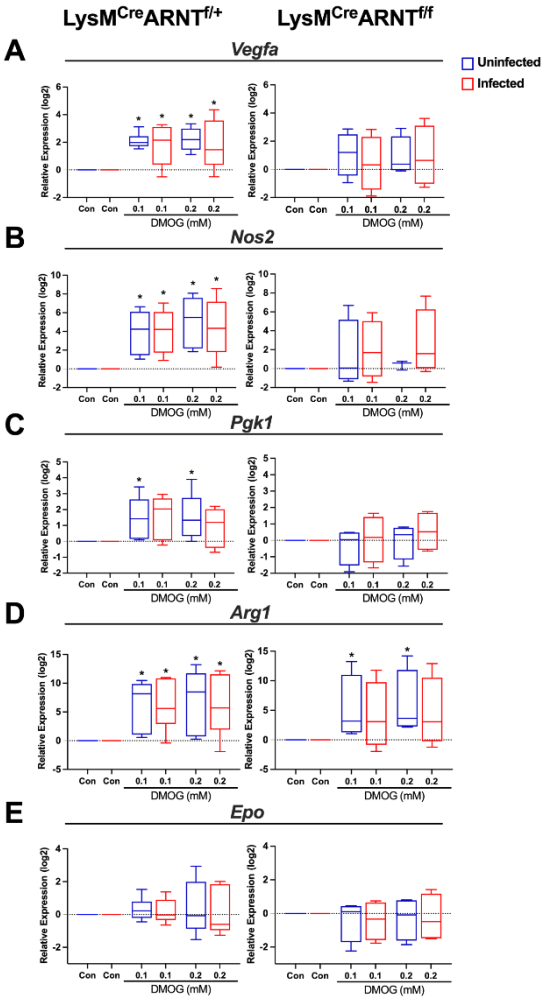

Figure 5. DMOG treatment induces HIF-1α and HIF-2α activation during L. major infection. BMDMs were generated from LysM^{Cre}ARNT$^{f/+}$ or LysM^{Cre}ARNT$^{f/f}$ mice. Macrophages were infected or not with *L. major* parasites (5:1 MOI) and cultured with and without 0.1 mM or 0.2 mM DMOG for 24 hours. The expression of *Vegfa* **(A)**, *Nos2* **(B)**, *Pgk1* **(C)**, *Arg1* **(D)**, and *Epo* **(E)** was analyzed by quantitative real-time PCR. Relative mRNA expression was normalized to the housekeeping gene *RpsII*. Results shown here are the mean +SEM of the fold change over untreated controls (Con) pooled from 4-6 individual experiments. *$p \leq 0.05$, Mann-Whitney test, comparing infected DMOG-treated to infected untreated controls (blue to blue), or comparing uninfected DMOG-treated to uninfected untreated controls (orange to orange).

2.6 Macrophage HIF-α deletion and stabilization during L. major internalization and killing

Given DMOG induces transcripts involved in parasite persistence like *Arg1* indicative of an M2 macrophage, and parasite killing like *Nos2* indicative of a M1 pro-inflammatory macrophage simultaneously, we analyzed parasite persistence in macrophages by monitoring parasite internalization as well as their growth and survival in macrophages with and without DMOG treatment. To determine if HIF-α stabilization impacts the ability of macrophages to phagocytose *L. major* parasites, C57BL/6 BMDM were treated with DMOG prior to infection. We found an equal number of parasites per macrophage after 2 hours of infection in DMOG-treated cells compared to untreated macrophages suggesting HIF-α stabilization does not impact macrophage phagocytosis of *L. major* parasites (Figure 6A). To determine if HIF-α stabilization impacts parasite killing, BMDM were infected and then treated with DMOG for the duration of infection. As we previously reported, DMOG treatment does not impact parasite growth in macrophages for the first 72 hours of infection (Figure 6B). Although LPS and IFNγ leads to parasite killing resulting in lower numbers of parasites after 72 hours, DMOG treatment does not impact the effects of LPS and IFNγ (Figure 6B).

Preprints (www.preprints.org) | NOT PEER-REVIEWED | Posted: 7 October 2021 doi:10.20944/preprints202110.0117.v1

While HIF-α stabilization did not affect host-parasite interactions in the first 72 hours, we wanted to determine if the absence of HIF-α signaling affects host-parasite interactions early during infection. BMDMs from LysM^{Cre}ARNT$^{f/f}$ and LysM^{Cre}ARNT$^{f/+}$ mice were infected and internalized *L. major* parasites were quantified after 2 hours. Surprisingly, LysM^{Cre}ARNT$^{f/f}$ macrophages possessed a significantly higher number of parasites per macrophage compared to LysM^{Cre}ARNT$^{f/+}$ macrophages, independent of DMOG treatment (Figure 6C). These data show that macrophages deficient in ARNT/HIF-α signaling exhibit higher numbers of phagocytosed parasites at 2 hours. After 72 hours p.i., parasite numbers were higher in LysM^{Cre}ARNT$^{f/f}$ macrophages compared to LysM^{Cre}ARNT$^{f/+}$ controls, irrespective of DMOG treatment (Figure 6D). LysM^{Cre}ARNT$^{f/f}$ macrophages exposed to LPS and IFNγ resulted in lower numbers of parasites when compared to untreated LysM^{Cre}ARNT$^{f/f}$ macrophages suggesting macrophages deficient in ARNT/HIF-α signaling can control parasites upon pro-inflammatory stimulation (Figure 6D). However, LysM^{Cre}ARNT$^{f/f}$ macrophages possessed a higher number of parasites per macrophage compared to LysM^{Cre}ARNT$^{f/+}$ controls following LPS and IFNγ stimulation indicating LysM^{Cre}ARNT$^{f/f}$ macrophages do exhibit a slight, yet significant, defect in their ability to kill parasites (Figure 6D, significant by *t*-test but not depicted on graph). Taken together, our findings show macrophage HIF-α stabilization does not impact parasite phagocytosis or killing, but ARNT/HIF-α signaling restricts parasite entry into macrophages.

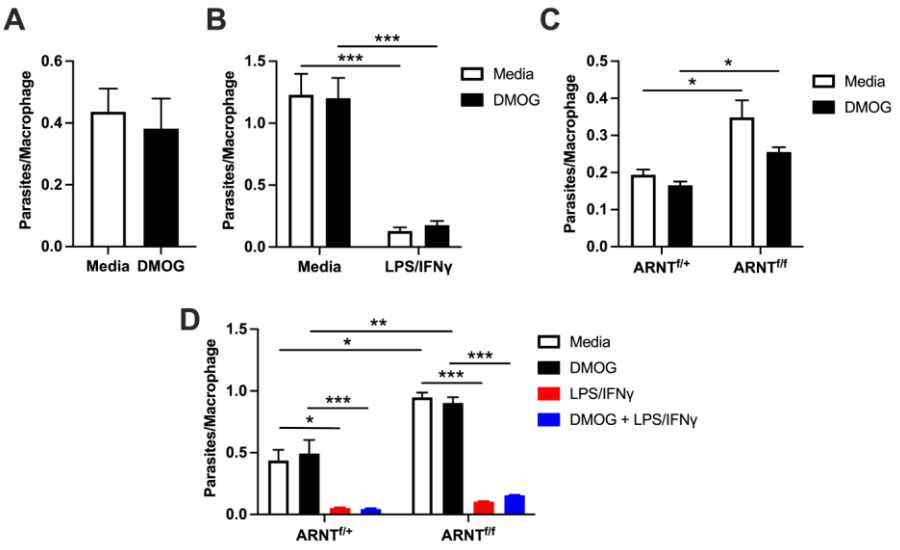

Figure 6. HIF-α stabilization does not impact parasite burdens in macrophages following L. major infection. For all experiments the number of parasites per macrophage was quantified by fluorescence microscopy. **(A)** C57BL/6 BMDM were pretreated overnight with or without 0.2 mM DMOG before infection with fluorescently-labelled DsRed *L. major* parasites (MOI 5:1). Parasites were quantified at 2 hours p.i. **(B)** C57BL/6 BMDM were infected with DsRed *L. major* and cultured for 72 hours with or without 0.2 mM DMOG in the presence or absence of 100 ng/mL LPS + 10 ng/mL IFNγ. **(C)** BMDM derived from LysM^{Cre}ARNT$^{f/+}$ and LysM^{Cre}ARNT$^{f/f}$ mice were pretreated overnight with and without 0.2 mM DMOG before being infected with DsRed *L. major* for 2 hours. **(D)** LysM^{Cre}ARNT$^{f/+}$ and LysM^{Cre}ARNT$^{f/f}$ BMDM were cultured for 72 hours after infection with or without 0.2 mM DMOG in the presence or absence of 100 ng/mL LPS + 10 ng/mL IFNγ. Results shown in A-B are pooled from 4 individual experiments. Results shown in C-D are a single experiment representative of 3-4 individual experiments. Data presented as the mean +SEM. **p* < 0.05, ***p* < 0.01 and ****p* < 0.005, *t-test* comparing DMOG and LPS/IFNγ treatment to media alone and conditioned media, or *t-test* comparing LysM^{Cre}ARNT$^{f/+}$ and LysM^{Cre}ARNT$^{f/f}$ macrophages under the same treatment conditions.

Preprints (www.preprints.org) | NOT PEER-REVIEWED | Posted: 7 October 2021 doi:10.20944/preprints202110.0117.v1

3. Discussion

During *L. major* infection myeloid cells including monocytes are recruited to dermal lesions where they experience hypoxic conditions. Our data shows the longevity of myeloid cells in the inflamed tissue enhances their hypoxic state. We find the hypoxic environment in leishmanial lesions is associated with the activation of HIF-α signaling. Given monocytes differentiate into macrophages at the site of infection, and HIF-α activation can impact macrophage function, we investigated the role of HIF-α signaling using a combination of strategies to augment and delete HIF-α activation during *L. major* infection. Upon infection, macrophages become activated to phagocytize and kill parasites by NO and ROS. However, macrophages also serve as the host cell and replicative niche for parasites. Macrophages also orchestrate lymphatic remodeling for lesion resolution. Therefore, macrophages play multiple roles in both parasite control and persistence as well as wound healing in CL. Altogether, we found pharmacological HIF-α activation promoted the ability of macrophages to drive lymphatic remodeling through VEGF-A production during infection, but HIF-α activation did not impact parasite phagocytosis or killing. Alternatively, basal HIF-α signaling restricted macrophage parasite phagocytosis. While HIF-α stabilization did not enhance parasite killing, our findings suggest pharmacological activation of HIF-α could induce VEGF-A which would be beneficial for promoting lymphangiogenesis to improve lesion resolution during CL.

Hypoxia promotes macrophage phagocytosis in a HIF-1α-dependent manner; while, HIF-2α is not involved in phagocytosis under hypoxic conditions [23]. In this study, we detected higher numbers of internalized parasites in macrophages deficient in myeloid ARNT/HIF-α signaling compared macrophages with intact ARNT/HIF-α signaling in normoxic conditions. These data suggest HIF-α inhibits parasite phagocytosis. While HIF-2α may not participate in phagocytosis under hypoxic conditions, basal HIF-2α is necessary and sufficient to suppress phagocytosis and efferocytosis under normoxic conditions [24]. The uptake of apoptotic cells or *Staphylococcus aureus* is higher in $LysM^{Cre}HIF\text{-}2\alpha^{f/f}$ macrophages compared to controls [24]. Moreover, $LysM^{Cre}ARNT^{f/f}$ macrophages (missing both HIF-1α and HIF-2α signaling like the macrophages used in our experiments) show enhanced phagocytosis and efferocytosis compared to control macrophages [24]. As a result, we hypothesize the absence of HIF-2α in our $LysM^{Cre}ARNT^{f/f}$ macrophages is responsible for the enhanced parasite uptake during *L. major* infection. Therefore, we propose HIF-2α acts as a phagocytic repressor during *Leishmania* infection.

HIF-α stabilization leads to lower bacterial and fungal burdens within macrophages [25, 26]. Complementing the work of others, our data show inflammatory stabilization of HIF-α by LPS and IFNγ promotes parasite killing but chemical HIF-α stabilization by DMOG treatment does not lead to parasite killing [6, 18]. HIF-α stabilization can occur by two major mechanisms including inhibiting prolyl hydroxylase (PHD) enzymes or factor inhibiting HIF (FIH) [27]. While previous studies stabilized HIF-α by inhibiting PHD enzymes without affecting FIH [6], we stabilize HIF-α by DMOG treatment, which inhibits both PHD enzymes and FIH, and showed chemical HIF-α stabilization alone does not induce parasite killing in the absence of additional pro-inflammatory stimuli. Therefore, our body of work continues to support the hypothesize that multiple factors from the tissue microenvironment like hypoxia and pro-inflammatory cytokines contribute to parasite killing. However, the requirement for HIF-α signaling in parasite killing is not completely clear. While it has been reported that myeloid HIF-1α is required for the robust killing of *L. major* parasites in a NO-dependent manner, we found ARNT/HIF-α signaling only plays a minor, although significant, role in parasite killing. Given $LysM^{Cre}ARNT^{f/f}$ macrophages could efficiently kill parasites in response to LPS and IFNγ, our data suggest *L. major* parasites are controlled in an ARNT/HIF-α-independent mechanism in vitro. Mice deficient in myeloid HIF-1α exhibit higher parasite numbers following *L. major* infection in vivo, but we did not detect differences in parasite burdens in infected $LysM^{Cre}ARNT^{f/f}$ mice, which are deficient in both myeloid HIF-1α and HIF-2α signaling [6, 18]. Our in vitro findings here showing $LysM^{Cre}ARNT^{f/f}$ macrophages can kill parasites in response to pro-inflammatory stimuli are consistent with our findings in vivo showing $LysM^{Cre}ARNT^{f/f}$ mice can control parasites at similar levels to $LysM^{Cre}ARNT^{f/+}$ controls [8, 18]. Altogether, these data suggest HIF-α signaling may contribute to parasite control following exposure to pro-inflammatory stimuli, but parasite killing occurs predominantly through HIF-α-independent mechanism.

While it is clear that HIF-α subunits are active during infection, the specific factors responsible for HIF-α activation have not been defined and appear to be context dependent. Hypoxia is hypothesized to be a major driver of HIF-α activation, but pro-inflammatory signals can also activate HIF-1α and HIF-2α [28, 29]. Here, we used VEGF-A production as a surrogate for HIF-α activation during infection. *L. major* parasites can activate TLRs and TLR activation can lead to HIF-α activation [30-34]. Similarly, *L. major* induces reactive oxygen species (ROS) production and ROS can activate HIF-α [35-38], but parasites alone did not induce VEGF-A production by macrophages. These data suggest parasites, parasite TLR ligation, and parasite-induced ROS production do not contribute to HIF-α activation during infection in vitro. We tested LPS and IFNγ alone and in combination given their known roles in stimulating pro-inflammatory M1 macrophages. We also predict macrophages are exposed to these molecules during *L. major* infection. LPS may activate skin macrophages during CL given the presence of the microbiome and the compromised integrity of the skin [39]. IFNγ is also elevated at the site of infection due to the host Th1 immune response [3]. While pro-inflammatory stimuli have been hypothesized to induce HIF-α activation, we did not find these factors to be robust drivers of macrophage VEGF-A production. As a result, we speculate hypoxia or other soluble mediators in the inflamed skin drive HIF-α activation and VEGF-A production by macrophages during *L. major* infection. VEGF-A can also be induced by a variety of growth factors and cytokines including FGF2, PDGF, TGF-β, IL-1β, IL-6, IL-8/CXCL8, TNFα, and some of these soluble mediators act synergistically with hypoxia [40-47]. Importantly, many of these factors are present in leishmanial lesions and may induce VEGF-A during *L. major* infection. As a result, the identification of the factors responsible for VEGF-A production by macrophages is the focus of ongoing investigation in the lab given the critical role of VEGF-A in lesion resolution during CL.

4. Materials and Methods

4.1 Mice

Female and male animals used in these experiments were either purchased from the National Cancer Institute or bred in a vivarium on campus. CD45.2$^+$ C57BL/6 and CD45.1$^+$ C57BL/6 mice were purchased from the National Cancer Institute. Mice with a myeloid-specific *ARNT* conditional knockout were bred by crossing a strain expressing the LysM^{Cre} allele with a strain with a floxed *ARNT* conditional allele [48, 49]. The LysM^{Cre}ARNT$^{f/f}$ and LysM^{Cre}ARNT$^{f/+}$ control mice were a gift from M. Celeste Simon (University of Pennsylvania, Philadelphia, PA). LysM^{Cre}ARNT$^{f/f}$ mice were infected alongside LysM^{Cre}ARNT$^{f/+}$ controls for experiments. All mice were housed in vivariums under pathogen-free conditions at the University of Arkansas for Medical Sciences (UAMS). All infections were done on mice between 6 and 8 weeks of age. All procedures performed were approved by UAMS IACUC and followed institutional guidelines.

4.2 Parasites

Leishmania major and DsRed *L. major* Friedlin strain parasites were grown *in vitro* in Schneider's insect media (Gibco), supplemented with 20% heat-inactivated fetal bovine serum (FBS, Invitrogen), 100 U/mL penicillin and 100 U/mL streptomycin, and 2 mM L-glutamine (MilliporeSigma). Metacyclic promastigotes used for infections were isolated from 4-5 day old cultures using Ficoll gradient separation (MilliporeSigma) [50].

4.3 *In vivo* infections

Infections were performed by injecting 2x10^6 parasites in 10 μL of PBS intradermally into the right ear of mice. Mice were anesthetized with ketamine and xylazine prior to infection. Lesion development was monitored weekly by measuring of ear thickness, lesion diameter, and pathology to calculate lesion volume. Ears were digested for 90 minutes at 37^{o}C with 0.25 mg/mL liberase TL (Roche) with 10 μg/mL DNase I (Sigma) in RPMI 1640 media (Gibco).

4.4 Isolation of CD11b$^+$ cells and adoptive transfer

Spleens, femurs, tibias, and fibulas were taken from C57BL/6 mice to obtain bone marrow cells. Single cell suspensions were enriched using a CD11b MicroBead isolation kit (Miltenyi Biotec) to obtain myeloid cells. For positive selection, the autoMACS Pro Separator (Miltenyi) was used. CD11b$^+$ cells from the bone marrow (purity >97%) were resuspended in PBS and 4x10^6 cells were injected into the retroorbital sinus of the recipient C57BL/6 mouse.

Preprints (www.preprints.org) | NOT PEER-REVIEWED | Posted: 7 October 2021 doi:10.20944/preprints202110.0117.v1

4.5 Flow cytometry

Surface staining were performed on dermal cells from ears after enzymatic digestion and processing. To exclude dead cells, cell suspensions were first incubated with LIVE/DEAD Fixable Aqua Dead cell dye (Invitrogen) for 10 min at room temperature. FcγRs were blocked with 2.4G2 anti-mouse CD16/32 antibody (BioXCell) and 0.2% normal rat IgG (BioXCell) for 10 min at 4° C. For surface staining, cells were stained for 30 min at 4° C using antibodies: anti-CD45 AF 700 (clone 30-F11), anti-CD45.1 eFlour450 (clone A20), anti-CD45.2 AF 700 (clone 104), anti-Ly6C PerCpCy5.5 (clone HK1.4) (all from eBiosciences); anti-CD11b BV605 (clone M1/70), anti-Ly6G APC (clone 1A8), anti-CD64 PECy7 (clone X54-5/7.1) (all from Biolegend) in the presence of Brilliant Violet Buffer (BD Biosciences) or Super Bright staining buffer (eBiosciences). Cell events were acquired using the LSRII Fortessa flow cytometer (BD Biosciences) and analyzed using FlowJo software Version 10 (Tree Star).

4.6 Pimonidazole

Each mouse was injected with 1.5 mg pimonidazole (Hypoxyprobe kit) in 200 μL PBS intraperitoneally (i.p.) 90 min before sacrifice to measure hypoxia at the cellular level. Cells were fixed and permeabilized using the Foxp3 intracellular staining kit (eBiosciences) after cell-surface staining. Intracellular staining was carried out with α-pimonidazole-FITC (1:100) according to the manufacturer's instructions.

4.7 mRNA extraction and real-time PCR

mRNA was extracted using the EZNA Total RNA Kit I (Omega BioTek) and reverse transcribed using high-capacity cDNA Reverse Transcription (Applied Biosystems). Quantitative real-time PCR (qPCR) was performed on a QuantStudio 6 Flex Real-Time PCR system (Life Technologies) with SYBR Green PCR Master Mix. qPCR results were normalized to the housekeeping gene ribosomal protein S11 (RPS11) with a comparative threshold cycling method ($2^{-\Delta\Delta CT}$) to quantify. The following mouse primers were selected from Harvard's Primer Bank (https://pga.mgh.harvard.edu/primerbank/): *Vegfa* (Forward 5'-ATCTTCAAGCCGTCCTGTGT-3' and Reverse 5'-GCATTCACATCTGCTGTGCT-3'), *Nos2* (Forward 5'- ATGGAGACTGTCCCAGCAAT -3' and Reverse 5' - GGCGCAGAACTGAGGGTA -3'), *Epo* (Forward 5'- CATCTGCGACAGTCGAGTTCTG -3' and Reverse 5' - CACAACCCATCGTGACATTTTC -3'), *Pgk1* (Forward 5'-ATGTCGCTTAACAAGCTG -3' and Reverse 5'-GCTCCATTGTCCAAGCAGAAT -3'), *Arg1* (Forward 5'-CTCCAAGCCAAAGTCCTTAGAG -3' and Reverse 5'-AGGAGCTGTCATTAGGGACATC -3'), and *Rps11* (Forward 5'-CGTGACGAAGATGAAGATGC-3' and Reverse 5'-GCACATTGAATCGCACAGTC-3').

4.8 RNA Sequencing (RNASeq): data analysis

Following demultipexing, RNA reads were surveyed for sequencing quality using FastQC (version 1.7) (http://www.bioinformatics.babraham.ac.uk/projects/fastqc) and MultiQC (version 1.6) [51]. Next, the raw reads were processed according to Lexogen's QuantSeq data analysis pipeline with slight modification. Residual 3' adapters, polyA read through sequences, and low quality (Q < 20) bases were trimmed using BBTools BBDuk (version 38.52) (https://sourceforge.net/projects/bbmap/). Additionally, first 12 bases were also removed per the manufacture's suggestion. Cleaned reads (≥ 20 bp) were mapped to the mouse reference genome (GRCm38/mm10/ensemble release-84.38/ GCA_000001635.6) using STAR (version 2.6.1a), permitting up to 2 mismatches depending on the alignment length (e.g. 0 mismatches for 20-29 bp; 1 mismatch for 30-50 bp; 2 mismatches for 50-60+ bp) [52]. Reads mapping to > 20 locations were discarded. Gene level counts were quantified using HTSeq (htseq-counts) (version 0.9.1) (mode:intersection-nonempty) [53]. Genes with unique Entrez IDs and at least ~2 counts-per-million (CPM) in 4 or more samples were chosen for statistical testing. Next, scaling normalization using the trimmed mean of M-values (TMM) method was used to correct for compositional differences between sample libraries [54]. Differential expression was assessed using limma voomWithQualityWeights function with empirical bayes smoothing [55]. Genes with Benjamini & Hochberg adjusted p-values ≤ 0.05 and fold-changes ≥ 2 were considered significant [56]. Gene set enrichment analysis (GSEA) using Kyoto Encyclopedia of Genes and Genomes (KEGG) signaling pathways was carried out using EGSEA with default parameters [57].

4.9 Generation of bone marrow-derived macrophages

Femurs were removed from mice and soaked in 70% ethanol for 2 minutes then flushed with 10 mL cDMEM. The cells were resuspended, counted, and plated 5 x 10^6/mL in a 100 mm petri dish in 10 mL of conditioned macrophage media (cDMEM with 25% of L929 cell supernatants) for 7 days. At day 3 of 7, an additional 10 mL of conditioned macrophage media is added to each petri dish. At day 7, the cells were washed with ice cold PBS and harvested by dislodging by pipetting and a cell scraper. The cells were then pooled and counted to plate into either 24 well plates (1x10^6 cells in 1 mL) or 48 well plates (5x10^5 cells in 500 µL).

4.10 *In vitro* infections with DMOG treatment

Bone marrow-derived macrophages (BMDMs) were plated as described above into 24 well plates for overnight. Macrophages were cultured with *L. major* parasites (MOI 5:1) and extracellular parasites were washed away after 2 hours. Following the washes, cells were cultured in triplicate with 100 ng/mL LPS (Sigma), 10 ng/mL IFNγ (Peprotech), with or without 0.1, 0.2, or 0.3 mM DMOG (Sigma) for 2, 24, or 72 hours. Pretreated macrophages were incubated for overnight with DMOG prior to infection.

4.11 Microscopy for parasite quantification in vitro

After infection with DsRed *L. major* parasites, BMDMs were stained by removing conditioned media from each well and washing with PBS before fixation by methanol at -20 °C for 3 minutes. After fixation, the methanol was removed and the wells washed twice with PBS before staining with DAPI in PBS (Invitrogen) for 5 minutes in the dark at room temperature. After staining, the DAPI solution was removed and the wells again washed twice with PBS. After washing, 500 µL of PBS was added to each well to keep the cells hydrated. The plate then was wrapped in aluminum foil and stored in a 4 °C refrigerator. Fluorescence imaging was performed on a Keyence BZ-X810 using the 20X Plan-Fluor NA 0.45 objective in high resolution mode. Five images were taken at random locations in each well in both the DAPI and DsRed/TxRed channels. Cell counts were recorded using the BZ Image Analyzer (Keyence). Parasite counts were normalized to macrophage number by dividing the average number of parasites by the average number of macrophages for an individual well.

4.12 VEGF-A production

Cell free supernatants were collected at 24 hours following parasite infection to measure VEGF-A production using the Mouse VEGF-A ELISA kit according to manufacturer's instructions (R and D Systems).

4.13 Statistics

All data were analyzed using GraphPad Prism 8 or 9, and $p \leq 0.05$ was considered statistically significant. Statistical significance was calculated using a 2-tailed Student's unpaired or paired *t-test* for a single comparison between groups. A Grubbs' test was used to identify and mathematically remove outlier data points. For multiple-comparison analysis, statistical significance was determined by a one-way analysis of variance (ANOVA) followed by the post hoc Tukey's test with no designated control group, or a Mann-Whitney test with a designated control group.

Author Contributions: Conceptualization, T.W.; Methodology, M.B., H.R., A.B., S.D.B, and T.W.; Validation, M.B., H.R., A.B., L.F., S.M., H.W., and T.W.; Formal Analysis, M.B., H.R., A.B., G.V., C.L.W., L.F., S.M., H.W., S.D.B, and T.W.; Investigation, M.B., H.R., A.B., G.V., C.L.W., L.F., S.M., H.W., S.D.B, and T.W.; Writing – Original Draft Preparation, M.B., H.R., A.B., G.V., S.D.B., and T.W.; Writing – Review & Editing, M.B., H.R., A.B., G.V., C.L.W., L.F., S.M., H.W., S.D.B., and T.W.; Visualization, M.B., H.R., A.B., C.L.W., S.D.B, and T.W.; Project Administration, T.W.; Funding Acquisition, S.D.B. and T.W.

Funding: This research was funded by the Center for Microbial Pathogenesis and Host Inflammatory Responses (funded by National Institutes of Health National Institute of General Medical Sciences Centers of Biomedical Research Excellence Grant P20-GM103625) and the Oak Ridge Associated Universities (ORAU) 2019 Ralph E. Powe Junior Faculty Enhancement Award to Dr. Weinkopff. This work was also supported by the UAMS Translational Research Institute in collaboration with the UAMS Division for Diversity, Equity and Inclusion (DDEI) Mini Grants for Under-Represented Faculty Researchers to Dr. Weinkopff as part of the NIH National Center for Advancing Translational Sciences (NCATS), UL1 TR003107. Additionally, the work is supported by the Center for Translational Pediatric Research funded under the NIH grant P20GM121293. The funders had no role in study design, data analysis, decision to publish or preparation of the manuscript.

Institutional Review Board Statement: The study was conducted according to the guidelines of the Declaration of Helsinki, and approved by the Institutional Review Board of the University of Arkansas for Medical Sciences (animal protocol use 4013 approved on June 10, 2020).

Data Availability Statement: Data is contained within the article and the data from our bulk RNA-Seq analysis were deposited in Gene Expression Omnibus (GEO accession number – GSE185253).

Acknowledgments: We thank Andrea Harris from flow cytometry core facility, and veterinary staff from the Division of Laboratory Animal Medicine (DLAM) at UAMS for their excellent technical assistance.

Conflicts of Interest: The authors declare no conflict of interest. The funders had no role in the design of the study; in the collection, analyses, or interpretation of data; in the writing of the manuscript, or in the decision to publish the results.

References

1. Alvar J, Velez ID, Bern C, Herrero M, Desjeux P, Cano J, et al. Leishmaniasis worldwide and global estimates of its incidence. PLoS One. 2012;7(5):e35671. Epub 2012/06/14. doi: 10.1371/journal.pone.0035671. PubMed PMID: 22693548; PubMed Central PMCID: PMCPMC3365071.
2. Zhang WW, Karmakar S, Gannavaram S, Dey R, Lypaczewski P, Ismail N, et al. A second generation leishmanization vaccine with a markerless attenuated Leishmania major strain using CRISPR gene editing. Nat Commun. 2020;11(1):3461. Epub 2020/07/12. doi: 10.1038/s41467-020-17154-z. PubMed PMID: 32651371; PubMed Central PMCID: PMCPMC7351751.
3. Scott P, Novais FO. Cutaneous leishmaniasis: immune responses in protection and pathogenesis. Nat Rev Immunol. 2016;16(9):581-92. Epub 2016/07/19. doi: 10.1038/nri.2016.72. PubMed PMID: 27424773.
4. Postigo JA. Leishmaniasis in the World Health Organization Eastern Mediterranean Region. Int J Antimicrob Agents. 2010;36 Suppl 1:S62-5. Epub 2010/08/24. doi: 10.1016/j.ijantimicag.2010.06.023. PubMed PMID: 20728317.
5. Fraga CA, Oliveira MV, Alves LR, Viana AG, Sousa AA, Carvalho SF, et al. Immunohistochemical profile of HIF-1alpha, VEGF-A, VEGFR2 and MMP9 proteins in tegumentary leishmaniasis. An Bras Dermatol. 2012;87(5):709-13. Epub 2012/10/10. PubMed PMID: 23044562.
6. Schatz V, Strussmann Y, Mahnke A, Schley G, Waldner M, Ritter U, et al. Myeloid Cell-Derived HIF-1alpha Promotes Control of Leishmania major. J Immunol. 2016;197(10):4034-41. Epub 2016/11/01. doi: 10.4049/jimmunol.1601080. PubMed PMID: 27798163.
7. Weinkopff T, Konradt C, Christian DA, Discher DE, Hunter CA, Scott P. Leishmania major Infection-Induced VEGF-A/VEGFR-2 Signaling Promotes Lymphangiogenesis That Controls Disease. J Immunol. 2016;197(5):1823-31. Epub 2016/07/31. doi: 10.4049/jimmunol.1600717. PubMed PMID: 27474074; PubMed Central PMCID: PMCPMC5001553.
8. Weinkopff T, Roys H, Bowlin A, Scott P. Leishmania Infection Induces Macrophage Vascular Endothelial Growth Factor A Production in an ARNT/HIF-Dependent Manner. Infect Immun. 2019;87(11). Epub 2019/08/28. doi: 10.1128/IAI.00088-19. PubMed PMID: 31451620; PubMed Central PMCID: PMCPMC6803331.
9. Bowlin A, Roys H, Wanjala H, Bettadapura M, Venugopal G, Surma J, et al. Hypoxia-Inducible Factor Signaling in Macrophages Promotes Lymphangiogenesis in Leishmania major Infection. Infect Immun. 2021;89(8):e0012421. Epub 2021/05/26. doi: 10.1128/IAI.00124-21. PubMed PMID: 34031127; PubMed Central PMCID: PMCPMC8281282.
10. Degrossoli A, Bosetto MC, Lima CB, Giorgio S. Expression of hypoxia-inducible factor 1alpha in mononuclear phagocytes infected with Leishmania amazonensis. Immunol Lett. 2007;114(2):119-25. Epub 2007/11/07. doi: 10.1016/j.imlet.2007.09.009. PubMed PMID: 17983667.
11. Singh AK, Mukhopadhyay C, Biswas S, Singh VK, Mukhopadhyay CK. Intracellular pathogen Leishmania donovani activates hypoxia inducible factor-1 by dual mechanism for survival advantage within macrophage. PLoS One. 2012;7(6):e38489. Epub 2012/06/16. doi: 10.1371/journal.pone.0038489. PubMed PMID: 22701652; PubMed Central PMCID: PMCPMC3373497.
12. Arandjelovic S, Ravichandran KS. Phagocytosis of apoptotic cells in homeostasis. Nat Immunol. 2015;16(9):907-17. Epub 2015/08/20. doi: 10.1038/ni.3253. PubMed PMID: 26287597; PubMed Central PMCID: PMCPMC4826466.
13. Greenberg ME, Sun M, Zhang R, Febbraio M, Silverstein R, Hazen SL. Oxidized phosphatidylserine-CD36 interactions play an essential role in macrophage-dependent phagocytosis of apoptotic cells. J Exp Med. 2006;203(12):2613-25. Epub 2006/11/15. doi: 10.1084/jem.20060370. PubMed PMID: 17101731; PubMed Central PMCID: PMCPMC2118161.
14. Kima PE, Soong L, Chicharro C, Ruddle NH, McMahon-Pratt D. Leishmania-infected macrophages sequester endogenously synthesized parasite antigens from presentation to CD4+ T cells. Eur J Immunol. 1996;26(12):3163-9. Epub 1996/12/01. doi: 10.1002/eji.1830261249. PubMed PMID: 8977318.
15. Liu D, Uzonna JE. The early interaction of Leishmania with macrophages and dendritic cells and its influence on the host immune response. Front Cell Infect Microbiol. 2012;2:83. Epub 2012/08/25. doi: 10.3389/fcimb.2012.00083. PubMed PMID: 22919674; PubMed Central PMCID: PMCPMC3417671.
16. Meier CL, Svensson M, Kaye PM. Leishmania-induced inhibition of macrophage antigen presentation analyzed at the single-cell level. J Immunol. 2003;171(12):6706-13. Epub 2003/12/10. doi: 10.4049/jimmunol.171.12.6706. PubMed PMID: 14662874.
17. von Stebut E, Belkaid Y, Jakob T, Sacks DL, Udey MC. Uptake of Leishmania major amastigotes results in activation and interleukin 12 release from murine skin-derived dendritic cells: implications for the initiation of anti-Leishmania immunity. J Exp Med. 1998;188(8):1547-52. Epub 1998/10/23. doi: 10.1084/jem.188.8.1547. PubMed PMID: 9782133; PubMed Central PMCID: PMCPMC2213412.
18. Bowlin A, Roys H, Wanjala H, Bettadapura M, Venugopal G, Surma J, et al. Hypoxia inducible factor signaling in macrophages promotes lymphangiogenesis in Leishmania major infection. Infect Immun. 2021. Epub 2021/05/26. doi: 10.1128/IAI.00124-21. PubMed PMID: 34031127.

19. Zhdanov AV, Okkelman IA, Collins FW, Melgar S, Papkovsky DB. A novel effect of DMOG on cell metabolism: direct inhibition of mitochondrial function precedes HIF target gene expression. Biochim Biophys Acta. 2015;1847(10):1254-66. Epub 2015/07/06. doi: 10.1016/j.bbabio.2015.06.016. PubMed PMID: 26143176.
20. Leon B, Lopez-Bravo M, Ardavin C. Monocyte-derived dendritic cells formed at the infection site control the induction of protective T helper 1 responses against Leishmania. Immunity. 2007;26(4):519-31. Epub 2007/04/07. doi: 10.1016/j.immuni.2007.01.017. PubMed PMID: 17412618.
21. Petritus PM, Manzoni-de-Almeida D, Gimblet C, Gonzalez Lombana C, Scott P. Leishmania mexicana induces limited recruitment and activation of monocytes and monocyte-derived dendritic cells early during infection. PLoS Negl Trop Dis. 2012;6(10):e1858. Epub 2012/10/25. doi: 10.1371/journal.pntd.0001858. PubMed PMID: 23094119; PubMed Central PMCID: PMCPMC3475671.
22. Ribeiro-Gomes FL, Peters NC, Debrabant A, Sacks DL. Efficient capture of infected neutrophils by dendritic cells in the skin inhibits the early anti-leishmania response. PLoS Pathog. 2012;8(2):e1002536. Epub 2012/02/24. doi: 10.1371/journal.ppat.1002536. PubMed PMID: 22359507; PubMed Central PMCID: PMCPMC3280984.
23. Anand RJ, Gribar SC, Li J, Kohler JW, Branca MF, Dubowski T, et al. Hypoxia causes an increase in phagocytosis by macrophages in a HIF-1alpha-dependent manner. J Leukoc Biol. 2007;82(5):1257-65. Epub 2007/08/07. doi: 10.1189/jlb.0307195. PubMed PMID: 17675562.
24. Dehn S, DeBerge M, Yeap XY, Yvan-Charvet L, Fang D, Eltzschig HK, et al. HIF-2alpha in Resting Macrophages Tempers Mitochondrial Reactive Oxygen Species To Selectively Repress MARCO-Dependent Phagocytosis. J Immunol. 2016;197(9):3639-49. Epub 2016/09/28. doi: 10.4049/jimmunol.1600402. PubMed PMID: 27671111; PubMed Central PMCID: PMCPMC5101127.
25. Braverman J, Sogi KM, Benjamin D, Nomura DK, Stanley SA. HIF-1alpha Is an Essential Mediator of IFN-gamma-Dependent Immunity to Mycobacterium tuberculosis. J Immunol. 2016;197(4):1287-97. Epub 2016/07/20. doi: 10.4049/jimmunol.1600266. PubMed PMID: 27430718; PubMed Central PMCID: PMCPMC4976004.
26. Friedrich D, Zapf D, Lohse B, Fecher RA, Deepe GS, Jr., Rupp J. The HIF-1alpha/LC3-II Axis Impacts Fungal Immunity in Human Macrophages. Infect Immun. 2019;87(7). Epub 2019/05/01. doi: 10.1128/IAI.00125-19. PubMed PMID: 31036602; PubMed Central PMCID: PMCPMC6589057.
27. Sulser P, Pickel C, Gunter J, Leissing TM, Crean D, Schofield CJ, et al. HIF hydroxylase inhibitors decrease cellular oxygen consumption depending on their selectivity. FASEB J. 2020;34(2):2344-58. Epub 2020/01/08. doi: 10.1096/fj.201902240R. PubMed PMID: 31908020.
28. Imtiyaz HZ, Williams EP, Hickey MM, Patel SA, Durham AC, Yuan LJ, et al. Hypoxia-inducible factor 2alpha regulates macrophage function in mouse models of acute and tumor inflammation. J Clin Invest. 2010;120(8):2699-714. Epub 2010/07/21. doi: 10.1172/JCI39506. PubMed PMID: 20644254; PubMed Central PMCID: PMCPMC2912179.
29. Imtiyaz HZ, Simon MC. Hypoxia-inducible factors as essential regulators of inflammation. Curr Top Microbiol Immunol. 2010;345:105-20. Epub 2010/06/03. doi: 10.1007/82_2010_74. PubMed PMID: 20517715; PubMed Central PMCID: PMCPMC3144567.
30. Peyssonnaux C, Cejudo-Martin P, Doedens A, Zinkernagel AS, Johnson RS, Nizet V. Cutting edge: Essential role of hypoxia inducible factor-1alpha in development of lipopolysaccharide-induced sepsis. J Immunol. 2007;178(12):7516-9. Epub 2007/06/06. PubMed PMID: 17548584.
31. Zinkernagel AS, Hruz P, Uchiyama S, von Kockritz-Blickwede M, Schuepbach RA, Hayashi T, et al. Importance of Toll-like receptor 9 in host defense against M1T1 group A Streptococcus infections. J Innate Immun. 2012;4(2):213-8. Epub 2011/08/24. doi: 10.1159/000329550. PubMed PMID: 21860217; PubMed Central PMCID: PMCPMC3388268.
32. Halliday A, Bates PA, Chance ML, Taylor MJ. Toll-like receptor 2 (TLR2) plays a role in controlling cutaneous leishmaniasis in vivo, but does not require activation by parasite lipophosphoglycan. Parasit Vectors. 2016;9(1):532. Epub 2016/10/08. doi: 10.1186/s13071-016-1807-8. PubMed PMID: 27716391; PubMed Central PMCID: PMCPMC5053327.
33. Abou Fakher FH, Rachinel N, Klimczak M, Louis J, Doyen N. TLR9-dependent activation of dendritic cells by DNA from Leishmania major favors Th1 cell development and the resolution of lesions. J Immunol. 2009;182(3):1386-96. Epub 2009/01/22. doi: 10.4049/jimmunol.182.3.1386. PubMed PMID: 19155485.
34. Palazon A, Goldrath AW, Nizet V, Johnson RS. HIF transcription factors, inflammation, and immunity. Immunity. 2014;41(4):518-28. Epub 2014/11/05. doi: 10.1016/j.immuni.2014.09.008. PubMed PMID: 25367569; PubMed Central PMCID: PMCPMC4346319.
35. Salei N, Hellberg L, Kohl J, Laskay T. Enhanced survival of Leishmania major in neutrophil granulocytes in the presence of apoptotic cells. PLoS One. 2017;12(2):e0171850. Epub 2017/02/12. doi: 10.1371/journal.pone.0171850. PubMed PMID: 28187163; PubMed Central PMCID: PMCPMC5302790.
36. Filardy AA, Costa-da-Silva AC, Koeller CM, Guimaraes-Pinto K, Ribeiro-Gomes FL, Lopes MF, et al. Infection with Leishmania major induces a cellular stress response in macrophages. PLoS One. 2014;9(1):e85715. Epub 2014/01/15. doi: 10.1371/journal.pone.0085715. PubMed PMID: 24416445; PubMed Central PMCID: PMCPMC3887094.
37. Bonello S, Zahringer C, BelAiba RS, Djordjevic T, Hess J, Michiels C, et al. Reactive oxygen species activate the HIF-1alpha promoter via a functional NFkappaB site. Arterioscler Thromb Vasc Biol. 2007;27(4):755-61. Epub 2007/02/03. doi: 10.1161/01.ATV.0000258979.92828.bc. PubMed PMID: 17272744.
38. Masson N, Singleton RS, Sekirnik R, Trudgian DC, Ambrose LJ, Miranda MX, et al. The FIH hydroxylase is a cellular peroxide sensor that modulates HIF transcriptional activity. EMBO Rep. 2012;13(3):251-7. Epub 2012/02/09. doi: 10.1038/embor.2012.9. PubMed PMID: 22310300; PubMed Central PMCID: PMCPMC3323130.
39. Gimblet C, Meisel JS, Loesche MA, Cole SD, Horwinski J, Novais FO, et al. Cutaneous Leishmaniasis Induces a Transmissible Dysbiotic Skin Microbiota that Promotes Skin Inflammation. Cell Host Microbe. 2017;22(1):13-24 e4. Epub 2017/07/04. doi: 10.1016/j.chom.2017.06.006. PubMed PMID: 28669672; PubMed Central PMCID: PMCPMC5555377.
40. Ferrara N, Gerber HP, LeCouter J. The biology of VEGF and its receptors. Nat Med. 2003;9(6):669-76. Epub 2003/06/05. doi: 10.1038/nm0603-669. PubMed PMID: 12778165.
41. Seghezzi G, Patel S, Ren CJ, Gualandris A, Pintucci G, Robbins ES, et al. Fibroblast growth factor-2 (FGF-2) induces vascular endothelial growth factor (VEGF) expression in the endothelial cells of forming capillaries: an autocrine mechanism contributing

to angiogenesis. J Cell Biol. 1998;141(7):1659-73. Epub 1998/07/01. doi: 10.1083/jcb.141.7.1659. PubMed PMID: 9647657; PubMed Central PMCID: PMCPMC2132998.

42. Maloney JP, Gao L. Proinflammatory Cytokines Increase Vascular Endothelial Growth Factor Expression in Alveolar Epithelial Cells. Mediators Inflamm. 2015;2015:387842. Epub 2015/10/02. doi: 10.1155/2015/387842. PubMed PMID: 26424968; PubMed Central PMCID: PMCPMC4573992.
43. Nauck M, Roth M, Tamm M, Eickelberg O, Wieland H, Stulz P, et al. Induction of vascular endothelial growth factor by platelet-activating factor and platelet-derived growth factor is downregulated by corticosteroids. Am J Respir Cell Mol Biol. 1997;16(4):398-406. Epub 1997/04/01. doi: 10.1165/ajrcmb.16.4.9115750. PubMed PMID: 9115750.
44. Gary Lee YC, Melkerneker D, Thompson PJ, Light RW, Lane KB. Transforming growth factor beta induces vascular endothelial growth factor elaboration from pleural mesothelial cells in vivo and in vitro. Am J Respir Crit Care Med. 2002;165(1):88-94. Epub 2002/01/10. doi: 10.1164/ajrccm.165.1.2104006. PubMed PMID: 11779736.
45. Jeon SH, Chae BC, Kim HA, Seo GY, Seo DW, Chun GT, et al. Mechanisms underlying TGF-beta1-induced expression of VEGF and Flk-1 in mouse macrophages and their implications for angiogenesis. J Leukoc Biol. 2007;81(2):557-66. Epub 2006/10/21. doi: 10.1189/jlb.0806517. PubMed PMID: 17053163.
46. Hellwig-Burgel T, Rutkowski K, Metzen E, Fandrey J, Jelkmann W. Interleukin-1beta and tumor necrosis factor-alpha stimulate DNA binding of hypoxia-inducible factor-1. Blood. 1999;94(5):1561-7. Epub 1999/09/09. PubMed PMID: 10477681.
47. Martin D, Galisteo R, Gutkind JS. CXCL8/IL8 stimulates vascular endothelial growth factor (VEGF) expression and the autocrine activation of VEGFR2 in endothelial cells by activating NFkappaB through the CBM (Carma3/Bcl10/Malt1) complex. J Biol Chem. 2009;284(10):6038-42. Epub 2008/12/30. doi: 10.1074/jbc.C800207200. PubMed PMID: 19112107; PubMed Central PMCID: PMCPMC2649103.
48. Clausen BE, Burkhardt C, Reith W, Renkawitz R, Forster I. Conditional gene targeting in macrophages and granulocytes using LysMcre mice. Transgenic Res. 1999;8(4):265-77. Epub 2000/01/06. PubMed PMID: 10621974.
49. Lin N, Shay JES, Xie H, Lee DSM, Skuli N, Tang Q, et al. Myeloid Cell Hypoxia-Inducible Factors Promote Resolution of Inflammation in Experimental Colitis. Front Immunol. 2018;9:2565. Epub 2018/11/21. doi: 10.3389/fimmu.2018.02565. PubMed PMID: 30455703; PubMed Central PMCID: PMCPMC6230677.
50. Spath GF, Beverley SM. A lipophosphoglycan-independent method for isolation of infective Leishmania metacyclic promastigotes by density gradient centrifugation. Exp Parasitol. 2001;99(2):97-103. Epub 2001/12/26. doi: 10.1006/expr.2001.4656. PubMed PMID: 11748963.
51. Ewels P, Magnusson M, Lundin S, Kaller M. MultiQC: summarize analysis results for multiple tools and samples in a single report. Bioinformatics. 2016;32(19):3047-8. Epub 2016/06/18. doi: 10.1093/bioinformatics/btw354. PubMed PMID: 27312411; PubMed Central PMCID: PMCPMC5039924.
52. Dobin A, Davis CA, Schlesinger F, Drenkow J, Zaleski C, Jha S, et al. STAR: ultrafast universal RNA-seq aligner. Bioinformatics. 2013;29(1):15-21. Epub 2012/10/30. doi: 10.1093/bioinformatics/bts635. PubMed PMID: 23104886; PubMed Central PMCID: PMCPMC3530905.
53. Anders S, Pyl PT, Huber W. HTSeq--a Python framework to work with high-throughput sequencing data. Bioinformatics. 2015;31(2):166-9. Epub 2014/09/28. doi: 10.1093/bioinformatics/btu638. PubMed PMID: 25260700; PubMed Central PMCID: PMCPMC4287950.
54. Robinson MD, Oshlack A. A scaling normalization method for differential expression analysis of RNA-seq data. Genome Biol. 2010;11(3):R25. Epub 2010/03/04. doi: 10.1186/gb-2010-11-3-r25. PubMed PMID: 20196867; PubMed Central PMCID: PMCPMC2864565.
55. Liu R, Holik AZ, Su S, Jansz N, Chen K, Leong HS, et al. Why weight? Modelling sample and observational level variability improves power in RNA-seq analyses. Nucleic Acids Res. 2015;43(15):e97. Epub 2015/05/01. doi: 10.1093/nar/gkv412. PubMed PMID: 25925576; PubMed Central PMCID: PMCPMC4551905.
56. Benjamini Y, Hochberg Y. Controlling the False Discovery Rate - a Practical and Powerful Approach to Multiple Testing. J R Stat Soc B. 1995;57(1):289-300. doi: DOI 10.1111/j.2517-6161.1995.tb02031.x. PubMed PMID: WOS:A1995QE45300017.
57. Alhamdoosh M, Law CW, Tian L, Sheridan JM, Ng M, Ritchie ME. Easy and efficient ensemble gene set testing with EGSEA. F1000Res. 2017;6:2010. Epub 2018/01/16. doi: 10.12688/f1000research.12544.1. PubMed PMID: 29333246; PubMed Central PMCID: PMCPMC5747338.